POLITECNICO DI TORINO
Repository ISTITUZIONALE

Study Regarding the Tunability of a Frequency Selective Surface Having Incorporated Active Devices
and Control Network

(Article begins on next page)

26 December 2024

Study Regarding the Tunability of a Frequency Selective Surface Having Incorporated Active Devices and Control Network

Andrei-Marius Silaghi
Dept. of Measurements and Optical Electronics
Politehnica University Timisoara
Timisoara, Romania
andrei.silaghi@upt.ro

Catalin Pescari
Dept. of Measurements and Optical Electronics
Politehnica University Timisoara
Timisoara, Romania
catalin.pescari@upt.ro

Aldo De Sabata
Dept. of Measurements and Optical Electronics
Politehnica University Timisoara
Timisoara, Romania
aldo.de-sabata@upt.ro

Ladislau Matekovits
Dept. of Electronics and Telecommunications
Politecnico di Torino
Torino, Italy
ladislau.matekovits@polito.it

Andrei Neiconi
Dept. of Measurements and Optical Electronics
Politehnica University Timisoara
Timisoara, Romania
andrei.neiconi@upt.ro

Abstract—**The demand for tunable devices in modern communication networks is rising. This article proposes a design for a tunable frequency selective surface which has two states (simulating ON and OFF states of PIN diodes). In order to bias the active parts, PIN diodes are employed as active devices for tuning and control networks incorporated in the structures. The suggested designs have been evaluated using electromagnetic simulation. Parametric studies are done to enhance the tunability of the proposed structures.**

Keywords—FSS, parametric studies, PIN diodes, tunable

I. INTRODUCTION

Frequency selective surfaces (FSSs) are two-dimensional periodic structures that are employed in polarization conversion, shielding, spatial filtering, and other applications [1, 2]. Adding lumped elements to passive structures yields tunable versions counterparts since these designs need to adjust their response to meet various transmission and reflection requirements. PIN or varactor diodes are used in two of the proposed fundamental solutions [3, 4, 5]. Furthermore, the structures including active components must incorporate DC bias networks (Control network-CN) [5, 6].

This paper is organized as follows: a description of the proposed solution, including dimensions, placement of the diodes, and CNs, is given in Section II. In order to assess the procedure, initial results from full-wave electromagnetic simulations are also provided. A parametric study is carried out for the diodes in ON and OFF states in Sec. III, to illustrate the tuning capability. Conclusions are drawn lastly.

II. DESIGN OF THE INITIAL STRUCTURE

The asymmetric, cut-slot structure that some of the authors have previously introduced in [7] served as the starting point for the current designs: the presence of PIN diodes positioned across the cut-slots provides controlled geometry according to [8] (Fig. 1).

The top view of the unit-cell structure with metallic rectangular loadings constructed on an FR4 substrate layer, with $\varepsilon_r = 3.9$ and $\tan \delta = 0.025$, is shown in Fig. 1. The metallic areas are depicted in a gray color. The structure's thickness (z direction) is $h_1 = 1.58$ mm.

Figure 1 presents the geometrical dimensions of the structure. The edges of the unit cell are $D_u = 18$ mm and $D_v = 18$ mm. The dimensions of the large and small rectangles are $y_s = 14$ mm and $x_s = 12$ mm and $y_{ss} = 8$ mm and $x_{ss} = 6$ mm respectively. The lengths of the horizontal and vertical microstrip lines are 12 mm (x_m) and 14 mm (x_{m1}), respectively, and these two rectangles are joined by two cross lines having the same width, $y_m = 1$ mm. The outside horizontal lines are 0.35 mm wide, whereas the vertical lines have the same width as the two cross lines (1 mm).

As depicted in Fig. 1, cut-slots are inserted in order to place diodes appropriately. The width ($W_{cut} = 0.47$ mm) and length ($L_{cut} = 1$ mm) of the cut-slots are determined by the dimension of the diodes. The spacing between consecutive microstrip lines is 0.6 mm, and the dimensions of the microstrip lines on the ground face of the structure are $L_m = 18$ mm and $W_m = 0.4$ mm (Fig. 2).
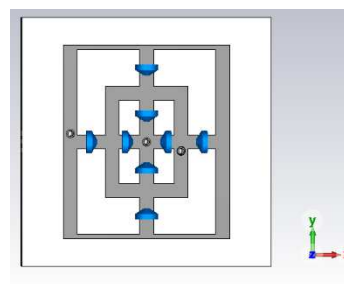

Fig. 1. Initial structure with diodes.

Moreover, feeding lines and the main structure are connected through via-holes (Fig. 2). The via-holes are positioned in the x direction away from the unit cell border as follows: the central via-hole is located at 9 mm, the right via-hole is at 6.5 mm, and the left via-hole is at 3.5 mm. Three parallel CN microstrip lines are shown in Fig. 2 as being connected through via holes to the main FSS structure in this area (one via hole connecting a single CN line to a metallic element of the structure) [7]. Previous research has examined how the introduction of CNs affects the periodic structure's functionality [7].
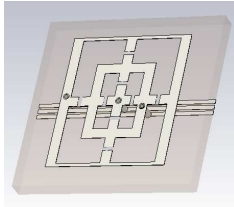
Fig. 2. Insight of CN lines.

The PIN diode's action, which effects the FSS's effectiveness, is determined by the applied bias voltage. PIN diodes act as capacitors (OFF state), when the structure is biased at a small voltage. Conversely, when the bias network is provided with a high voltage, the PIN diodes become a basically short circuit, which correlates to a low R (ON state) [5], [7].

The equivalent circuits for the PIN diodes ON and OFF states are shown in Fig. 3. The nominal values for the lumped elements, in the case of the PIN diodes acting as an *LC* circuit (OFF state), are: $L = 30$ pH, $C_s = 28$ fF, and $R_s = 30$ kΩ, while when the design actions as an *RL* circuit (ON state), the values switch to: $R_s = 7$ Ω and $L = 30$ pH [5], [8].
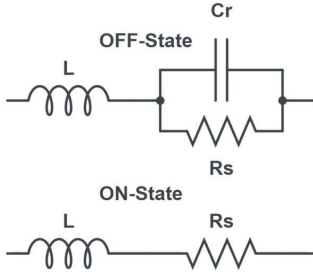

Fig. 3. Equivalent circuit for diodes states.

We have used the simulation tool [9] to compute the transmission coefficients in normal incidence for the diode structure in each of the ON and OFF states. First, the transmittance of the diode structure in the OFF-state for both the TE mode (blue color) and the TM mode (green color) is shown in Fig. 4. For the TE mode, resonances can be seen at 4.67 GHz, 9.8 GHz, and 11.9 GHz; for the TM mode, resonances occur at 2.76 GHz, 6.36 GHz, and 11.1 GHz [8].

In addition, the transmittance for the TE mode, when the diode structure is in the ON state, can be seen in Fig. 5. A stopband of -10 dB has been obtained between 6.51 GHz and 9.86 GHz in the case of TE incidence, which has a resonance located at 8.6 GHz. Additionally, between 10.18 GHz and 10.49 GHz and between 11.38 GHz and 11.71 GHz, two smaller bands are visible, centered at 10.29 GHz and 11.52 GHz respectively.
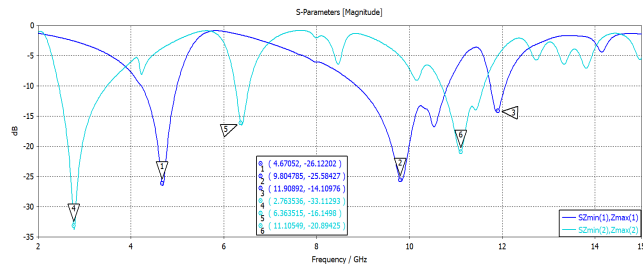

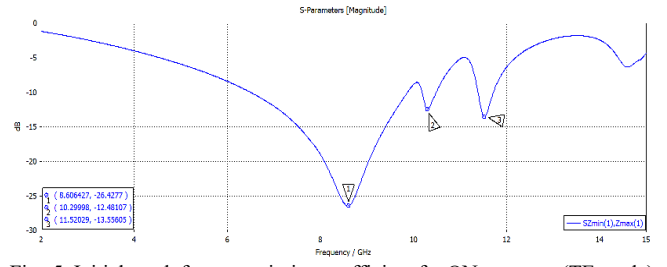Fig. 4. Initial result for transmission coefficient for OFF structure (modes TE and TM).

Fig. 5. Initial result for transmission coefficient for ON structure (TE mode).

III. PARAMETRIC STUDIES FOR THE STRUCTURES

A. OFF structure

A first parametric study was performed regarding the dimensions of the OFF-state structure. We started by reducing one dimension of the large rectangle from Fig. 1, namely x_s from 12 mm to 11 mm and then continued with reducing also one dimension from the smaller rectangle x_{ss} from 6 mm to 5 mm. The previously mentioned two results together with the initial one are depicted in Fig. 6. One can notice that in the lower frequency area, slight shift occurs as follows: from 4.68 GHz to 4.47 GHz (x_s) and to 4.43 GHz (x_{ss}) whereas a more drastic modification appears in the upper band: from 9.82 GHz to 9.61 GHz (x_s) and to 8.63 GHz (x_{ss}).

Moving on, having the dimensions obtained above, we also altered the y_{ss} parameter from 8 mm to 7 mm and then the y_m dimension from 1 mm to 0.3 mm (results visible in Fig. 7). By modifying y_{ss} there resulted no noticeable change around 4.4 GHz only around 8 GHz (8.63 GHz and 8.29 GHz), and the y_m parameter can shift from 4.4 GHz to 4.68 GHz, whilst at 8.6 GHz it remains almost the same (8.63 GHz and 8.69 GHz).
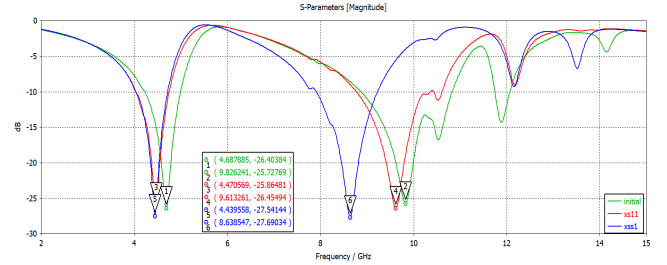

Fig. 6. Transmission result with modification of x_s and x_{ss} dimensions.
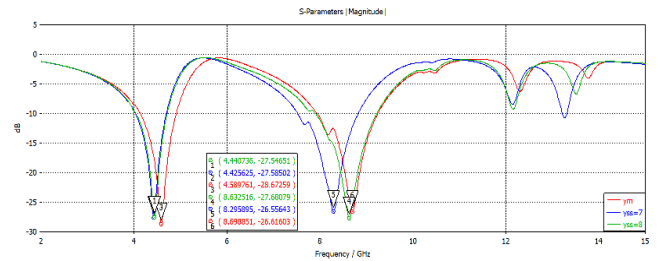

Fig. 7 Transmission result with modification of y_{ss} and y_m dimensions.

Next, with the previously obtained dimensions, we also modified the positions of the vias (results visible in Fig. 8). For example, the left-hand via hole has been moved from 3.5 mm to 3.75 mm and the right-hand via hole from 6.5 mm to 6.25 mm. This resulted in a modification of the frequency response in the lower frequency band: now, two notches appear at 4.45 GHz and 4.93 GHz and at 9.42 GHz respectively.

Furthermore, increasing the width of the microstrip line (W_m) from 0.4 mm to 0.5 mm had no effect on the frequency response of the structure.
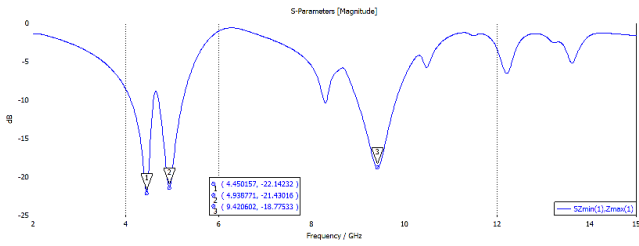

Fig. 8. Transmission result with via modification.

Another parametric study was performed regarding the dimensions of the working plane of the OFF-state structure: D_u and D_v have been both decreased from 18 and 18 mm (red color in Fig. 10) to 16 and 16 mm (blue color in Fig. 10). Via holes have been also displaced accordingly, so the new design is visible in Fig. 9. The comparison result is visible in Fig. 10.
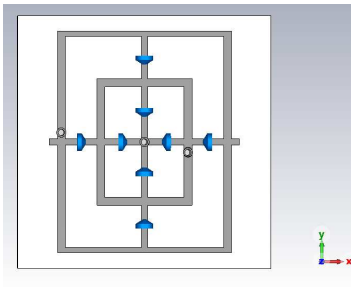

Fig. 9. Unit cell with modified dimensions.

In the initial scenario we obtained filtering between 4.1 and 5.23 GHz (with two notches present and centered at 4.45 and 4.94 GHz) and also between 8.97 and 9.82 GHz, the notch being at 9.41 GHz.

In the second scenario we obtained a different behavior. In the lower frequency range, we shifted a notch to 4.31 GHz and the second one remained at 4.94 GHz but with a different coefficient: -16.24 dB vs. -21.4 dB from the first scenario. Looking at the higher frequency range, we could move the second notch from 9.41 GHz to 9.75 GHz (having a -10dB stopband between 9.39 and 10.29 GHz).
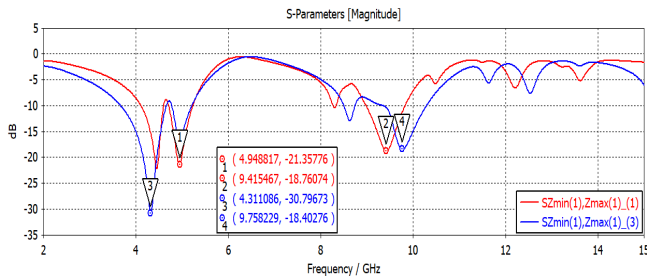

Fig. 10. D_u x D_v: 16x16 vs 18x18 initial.

In the next study D_u and D_v were both increased from 16 and 16 mm (blue color) to 20 and 20 mm (orange color). The comparison result is visible in Fig. 11.

In the first frequency range, the notch has been shifted to 4.98 GHz (-20.62dB) from 4.31 GHz (-31.01 dB), while in the upper frequency range, a more important change from 9.76 GHz (-18.41 dB) to 8.27 GHz (-22.96 dB) can be seen. Also, it is noticeable that with 20x20 mm² in the lower frequency band, a -10 dB stopband between 4.78 -5.11 GHz can be obtained, whereas in the higher band, the range 7.83-8.83 GHz has been obtained.
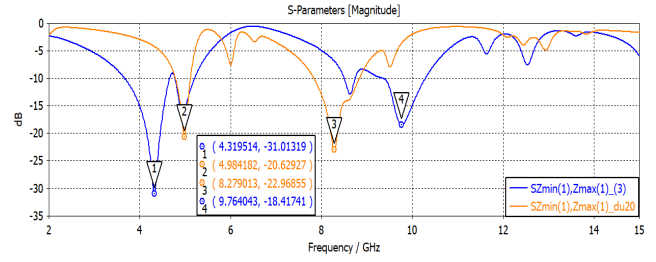

Fig. 11. D_u x D_v: 16.16 vs 20x20.

B. ON structure

The same geometrical modifications applied to the OFF-state structure (discussed in Fig. 6 - Fig. 8) were performed for the ON state structure as well. Then, the working plane dimensions were similar decreased from 18 mm to 16 mm. The results are visible in Fig. 12.

One can notice a shift in frequency for the main notch from 8.59 GHz to 6.98 GHz. The -10dB stopband also changes: 6.49 GHz – 9.87 GHz to 5.04 GHz – GHz 8.6 GHz.
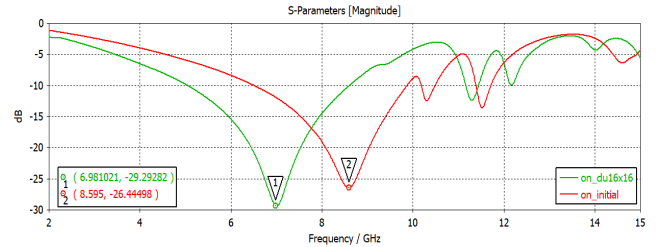

Fig. 12. Parametric study for the transmission results with ON state structure.

C. Angle variation

An investigation of the transmittance variability with the colatitude angle θ for both designs (OFF and ON states, with 16x16 working plane) has been considered. At first, an analysis in TE incidence was performed for the diode structure in the OFF state. The theta angle was varied in 15° increments from 0 to 45°. In Fig. 13, one can observe that the first notch (4.31 GHz) remains constant when θ increases, while the second notch is shifted towards lower frequencies from 9.75 GHz to 9.58 GHz.

For the design with the diodes in ON state, the transmittance variation is depicted in Fig. 14. One can notice that the main notch is shifted from 7.02 GHz (-29.28 dB) to 6.38 GHz (-29.36 dB) varying θ from 0 to 45°. Also, at 45° a new notch appears, centered at 8.59GHz (-24.69 dB).
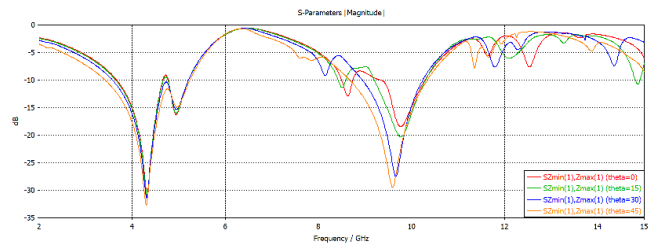

Fig. 13. Transmission results for OFF structure (TE mode), for different θ values.
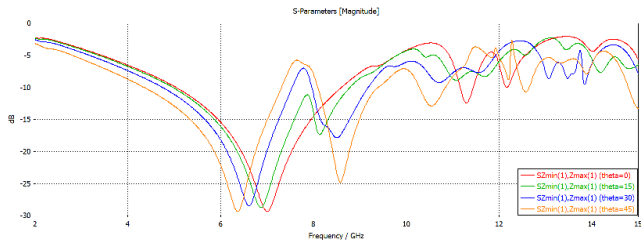
Fig. 14. Transmission results for ON structure (TE mode), for different θ values.

Afterwards, another investigation has been tackled, regarding the transmittance variability with the azimuth angle φ, keeping constant the colatitude angle θ for OFF state design. The φ angle was also varied in 15° increments from 0 to 45°, keeping θ angle at 0°. In Fig. 15 one can observe that the first notch shifts slightly when φ increases (from 4.31 GHz to 3.67 GHz), while the second notch turns into a wide band (9 GHz -10.2 GHz) having φ at 30° and 45°.
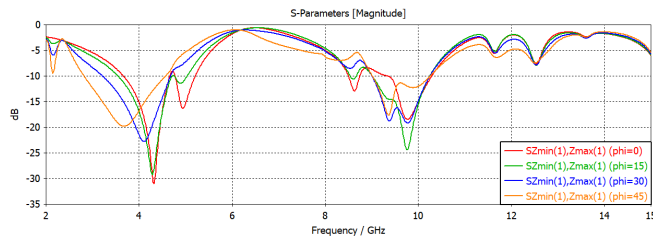

Fig. 15. Transmission results for OFF structure (TE mode), for different φ values (θ=0).

IV. CONCLUSIONS

This paper introduced a band-stop spatial filter for frequencies below 12 GHz, represented by a tunable FSS with multiple configurations. The tunability of the suggested designs has been demonstrated by two structures that displayed filtering and had diodes in both ON and OFF states, along with a control network. Parametric studies have been tackled to demonstrate the flexibility the FSSs provide for design.

REFERENCES

[1] B. A. Munk, Frequency Selective Surfaces: Theory and Design, NJ: Wiley, 2000.

[2] Natarajan, R.; Sivasamy, R.; Gunasekar, A., A compact polarization independent stop band frequency-selective surface for WLAN shielding. Microwave and Optical Technology Letters, 66(3), 2024.

[3] Azemi, S.N.; Ghorbani, K.; Rowe, W.S.T., A Reconfigurable FSS Using a Spring Resonator Element. IEEE Antennas Wirel. Propag. Lett. 2013, 12, 781–784.

[4] Zhang, L.; Yang, G.; Wu, Q.; Hua, J., A Novel Active Frequency Selective Surface with Wideband Tuning Range for EMC Purpose. IEEE Trans. Magn. 2012, 48, 4534–4537.

[5] Mir, F.; Matekovits, L.; De Sabata, A., Symmetry-breaking manipulation in the design of multifunctional tunable frequency selective surface. AEU Int. J. Electron. Commun. 2021, 142, 154003.

[6] Gao, X.; Yang,W.L.; Ma, H.F.; Cheng, Q.; Yu, X.H.; Cui, T.J., A Reconfigurable Broadband Polarization Converter Based on an Active Metasurface. IEEE Trans. Antennas Propag. 2018, 66, 6086–6095.

[7] Silaghi, A.-M.; Mir, F.; De Sabata, A.; Matekovits, L., Design and Experimental Validation of a Switchable Frequency Selective Surface with Incorporated Control Network. *Sensors* **2023**, *23*,4561. https://doi.org/10.3390/s23094561.

[8] Pescari, C.; Silaghi, A.-M.; De Sabata, A.; Matekovits, L.; Mir, F, Designing a Tunable Frequency Selective Surface with Active Components, 2024 IEEE International Symposium on Antennas and Propagation and ITNC-USNC-URSI Radio Science Meeting (APS 2024) (submited for publication)

[9] CST, Computer Simulation Technology (v2023), www.3ds.com.